

Modeling and control of inverter-based microgrids [★]

Bernhard Hammer ^{*} Kuangye Gong ^{*} Ulrich Konigorski ^{*}

^{*} TU Darmstadt, Landgraf-Georg-Str. 4, 64283 Darmstadt, Germany
(e-mail: bhammer@iat.tu-darmstadt.de).

Abstract: Assuming the most common control structure for zero and primary control of inverter-based microgrids, i.e. three cascades with the highest one being droop control, the potential benefit of optimizing the control parameters is investigated. A detailed nonlinear plant model is derived that compactly describes the dynamics in local dq-coordinates. Then, the design of the decentralized, cascaded controllers is converted into the problem of designing one centralized static controller with structural restrictions. To tune the controller parameters, a direct method for pole-assignment is used. The simulations show that the oscillations in the transient response can be reduced greatly by choosing appropriate control parameters, while the speed of the system is restricted due to the low-pass filtering of the power for primary control.

© 2018, IFAC (International Federation of Automatic Control) Hosting by Elsevier Ltd. All rights reserved.

Keywords: Microgrid, inverters, primary control, zero-level control, decentralized control, eigenstructure assignment

1. INTRODUCTION

The stability analysis of electricity grids has been of great research interest for a long time. Yet relatively few textbooks or publications actually treat the selection of the control parameters, and even fewer question the typically used control structure. This might be due to the fact that for large power systems the detailed model often is not available. But when considering microgrids, this should not be an issue. Another reason might be the difficulties arising due to the decentralized nature of grid control. And yet, the occurring problems have long been tackled by the control society, e.g. Litz (1983), Konigorski (1988), Siljak (1991), Lunze (1992).

Combining the modeling approaches broadly used in power system stability analysis and the results from the control society on the design of decentralized controllers, we tune the controller parameters of a microgrid to improve its transient behavior.

2. BASIC ASSUMPTIONS AND NOTATION

Assume a symmetrically constructed power system that is symmetrically operated. Then, only symmetrical signals occur. Let three-phase AC signals be written in vector notation: $\mathbf{x}_{abc} = (x_a \ x_b \ x_c)^T$. Let \mathcal{V}_N be the set of vertices and \mathcal{E}_N the set of edges of the network. Let $\mathcal{J} \subset \mathcal{V}_N$ be the set of vertices to which inverters are connected and $\mathcal{V}_L \subset \mathcal{V}_N$ the set of vertices to which loads are connected.

After power flow calculation, edges are added to represent the loads. Denote the set of these edges \mathcal{E}_L . They are connected to the ground node, which is the only element of \mathcal{V}_{L0} . The sets of vertices and edges of the resulting network used for the dynamical analysis are $\mathcal{V} = \mathcal{V}_N \cup \mathcal{V}_{L0}$ and $\mathcal{E} = \mathcal{E}_N \cup \mathcal{E}_L$. Let $|\bullet|$ be the cardinality of the set \bullet . We assume following numbering of the busses

$$\begin{aligned} \mathcal{J} &= \{1, \dots, |\mathcal{J}|\} \\ \mathcal{V}_L &= \{|\mathcal{J}| + 1, \dots, |\mathcal{J}| + |\mathcal{V}_L|\} \\ \mathcal{V}_N \setminus \mathcal{J} \cup \mathcal{V}_{L0} &= \{|\mathcal{J}| + |\mathcal{V}_L| + 1, \dots, |\mathcal{V}_N|\} \\ \mathcal{V}_{L0} &= \mathcal{V} \setminus \mathcal{V}_N = \{|\mathcal{V}_N| + 1\} = \{|\mathcal{V}|\} \end{aligned}$$

and of the edges

$$\begin{aligned} \mathcal{E}_N &= \{|\mathcal{V}| + 1, \dots, |\mathcal{V}| + |\mathcal{E}_N|\} \\ \mathcal{E}_L &= \mathcal{E} \setminus \mathcal{E}_N = \{|\mathcal{V}| + |\mathcal{E}_N| + 1, \dots, |\mathcal{V}| + |\mathcal{E}|\}. \end{aligned}$$

With this consecutive numbering of nodes and edges, currents injected into vertices and voltages at vertices, which have a subscript $i \in \mathcal{V}$, and voltages over edges and currents flowing through edges, which have a subscript $i \in \mathcal{E}$, can easily be distinguished. Let the subscripts $\mathcal{J}, \mathcal{V}_L, \mathcal{V}_N, \mathcal{V}_{L0}, \mathcal{V}, \mathcal{E}_N, \mathcal{E}_L, \mathcal{E}$ denote ordered column vectors from the corresponding set. For example, the voltages at the vertices are denoted $\mathbf{u}_{abc, \mathcal{V}}^T := [\mathbf{u}_{abc, 1}^T \ \dots \ \mathbf{u}_{abc, |\mathcal{V}|}^T]$. Define the function `diag`, which creates a diagonal matrix from its argument. Let the Kronecker product be denoted by \otimes , the Hadamard product by \circ and the inverse Hadamard product by $\mathbf{A}^{\circ(-1)} := (1/a_{ij})$. Define the dq-transformation

$$\mathbf{T}_{dq}(\theta) := \frac{\sqrt{2}}{\sqrt{3}} \begin{bmatrix} \cos(\theta) & \cos(\theta - \frac{2\pi}{3}) & \cos(\theta + \frac{2\pi}{3}) \\ -\sin(\theta) & -\sin(\theta - \frac{2\pi}{3}) & -\sin(\theta + \frac{2\pi}{3}) \end{bmatrix} \quad (1)$$

and the inverse dq-transformation

$$\mathbf{T}_{abc}(\theta) := \mathbf{T}_{dq}(\theta)^T \quad (2)$$

such that

This work is funded by the German [★] Federal Ministry for Economic Affairs and Energy under the support code 0324101.



$$\begin{aligned}\mathbf{x}_{dq} &= [x_d \ x_q]^T = \mathbf{T}_{dq}(\theta)\mathbf{x}_{abc} \\ \mathbf{T}_{abc}(\theta)\mathbf{x}_{dq} &= \mathbf{x}_{abc}.\end{aligned}\quad (3)$$

3. COORDINATE SYSTEMS

The coordinate systems are chosen as described in typical textbooks on the modeling of electricity networks, e.g. Kundur (1994), Anderson and Fouad (2003), Sauer and Pai (1997). The network will be described in dq-coordinates revolving with the angular velocity $\check{\omega}$. The transformation angle is

$$\theta = \text{mod}_{2\pi}(\check{\omega}t) \in \mathbb{T}, \quad (4)$$

where $\mathbb{T} := \{x \in \mathbb{R} | 0 \leq x < 2\pi\}$ and the operator $\text{mod}_{2\pi}$ is used so that $\theta \in \mathbb{T}$. Signals in network dq-coordinates will be underlined. Each inverter is described in its own $dq_{i \in \mathcal{J}}$ -coordinate system. The rotation frequencies $\omega_{i \in \mathcal{J}}$ of these local coordinate systems are set by the power controllers of the respective inverters. Then, the angle between the global network dq-coordinates and the local dq_i -coordinates can be tracked by integration

$$\delta_i(t) = \delta_{0,i} + \int_0^t (\omega_i(\tau) - \check{\omega})d\tau, \quad i \in \mathcal{J}, \quad (5)$$

where $\delta_{0,i}$ is the value of δ_i at $t = 0$. Since the signals in the final equations will be in local coordinates, signals in local coordinates will not specifically be marked. The transformation from local coordinates of inverter i to global coordinates is a rotation by δ_i

$$\mathbf{T}_{i \in \mathcal{J}} := \begin{bmatrix} \cos(\delta_i) & -\sin(\delta_i) \\ \sin(\delta_i) & \cos(\delta_i) \end{bmatrix}. \quad (6)$$

Define the block-diagonal transformation matrix

$$\mathbf{T}_{\mathcal{J}} := \text{diag}(\mathbf{T}_1, \dots, \mathbf{T}_{|\mathcal{J}|}). \quad (7)$$

Then, the voltages and currents at the inverter nodes can be transformed from local to global coordinates by

$$\mathbf{i}_{\mathcal{J}} = \mathbf{T}_{\mathcal{J}}\mathbf{i}_{\mathcal{J}}, \quad \mathbf{u}_{\mathcal{J}} = \mathbf{T}_{\mathcal{J}}\mathbf{u}_{\mathcal{J}}. \quad (8)$$

4. NETWORK MODEL

Let the electrical network be modeled by concentrated parameters. Conduct a power-flow calculation for a given operating point and compute the typical impedances as load models. To derive a dynamical model of the network with loads, we use the single-phase representation and Matlab's *power_statespace* command. This way, a state space model with voltages as input $\mathbf{u}_{a,\mathcal{J}}$ and currents as output $\mathbf{i}_{a,\mathcal{J}}$ is obtained:

$$\begin{aligned}\dot{\mathbf{x}}_a &= \mathbf{A}\mathbf{x}_a + \mathbf{B}\mathbf{u}_{a,\mathcal{J}} \\ \mathbf{i}_{a,\mathcal{J}} &= \mathbf{C}\mathbf{x}_a.\end{aligned}\quad (9)$$

Denote the order of the model n . First, extend the model to represent all three-phases

$$\begin{aligned}\dot{\mathbf{x}}_{abc} &= [\mathbf{A} \otimes \mathbf{I}_3] \mathbf{x}_{abc} + [\mathbf{B} \otimes \mathbf{I}_3] \mathbf{u}_{abc,\mathcal{J}} \\ \mathbf{i}_{abc,\mathcal{J}} &= [\mathbf{C} \otimes \mathbf{I}_3] \mathbf{x}_{abc}.\end{aligned}\quad (10)$$

Then, transform the model to global network dq-coordinates, which we denote by an underline, c.f. section 3. To do so, apply the inverse dq-transformation (3)

$$\begin{aligned}\dot{\underline{\mathbf{x}}}_{abc} &= [\mathbf{A} \otimes \mathbf{I}_3] [\mathbf{I}_n \otimes \mathbf{T}_{abc}] \underline{\mathbf{x}} \\ &\quad + [\mathbf{B} \otimes \mathbf{I}_3] [\mathbf{I}_{|\mathcal{J}|} \otimes \mathbf{T}_{abc}] \underline{\mathbf{u}}_{\mathcal{J}} \\ \underline{\mathbf{i}}_{abc,\mathcal{J}} &= [\mathbf{C} \otimes \mathbf{I}_3] [\mathbf{I}_n \otimes \mathbf{T}_{abc}] \underline{\mathbf{x}}\end{aligned}\quad (11)$$

and multiply the first equation of (11) by $\mathbf{I}_n \otimes \mathbf{T}_{dq}$ and the second equation by $\mathbf{I}_{|\mathcal{J}|} \otimes \mathbf{T}_{dq}$ from the left. Considering

the mixed-product property of the Kronecker-product, this leads to

$$\begin{aligned}[\mathbf{I}_n \otimes \mathbf{T}_{dq}] \dot{\underline{\mathbf{x}}}_{abc} &= [\mathbf{A} \otimes \mathbf{I}_2] \underline{\mathbf{x}} + [\mathbf{B} \otimes \mathbf{I}_2] \underline{\mathbf{u}}_{\mathcal{J}} \\ \underline{\mathbf{i}}_{\mathcal{J}} &= [\mathbf{C} \otimes \mathbf{I}_2] \underline{\mathbf{x}}.\end{aligned}\quad (12)$$

To compute $[\mathbf{I}_n \otimes \mathbf{T}_{dq}] \dot{\underline{\mathbf{x}}}_{abc}$ consider

$$\begin{aligned}\dot{\underline{\mathbf{x}}} &= \frac{d[\mathbf{I}_n \otimes \mathbf{T}_{dq}] \underline{\mathbf{x}}_{abc}}{dt} \\ &= \left[\mathbf{I}_n \otimes \begin{bmatrix} 0 & \check{\omega} \\ -\check{\omega} & 0 \end{bmatrix} \right] \underline{\mathbf{x}} + [\mathbf{I}_n \otimes \mathbf{T}_{dq}] \dot{\underline{\mathbf{x}}}_{abc}.\end{aligned}\quad (13)$$

Inserting (13) into (12) leads to

$$\begin{aligned}\dot{\underline{\mathbf{x}}} &= \left[\mathbf{A} \otimes \mathbf{I}_2 + \mathbf{I}_n \otimes \begin{bmatrix} 0 & \check{\omega} \\ -\check{\omega} & 0 \end{bmatrix} \right] \underline{\mathbf{x}} + [\mathbf{B} \otimes \mathbf{I}_2] \underline{\mathbf{u}}_{\mathcal{J}} \\ \underline{\mathbf{i}}_{\mathcal{J}} &= [\mathbf{C} \otimes \mathbf{I}_2] \underline{\mathbf{x}},\end{aligned}\quad (14)$$

which is the network model in dq-coordinates. Since the inverters will all be described in local dq-coordinates, transform input and output of (14) to local coordinates, too. Application of (8) yields

$$\begin{aligned}\dot{\underline{\mathbf{x}}} &= \tilde{\mathbf{A}}\underline{\mathbf{x}} + \tilde{\mathbf{B}}\mathbf{T}_{\mathcal{J}}(\delta_{\mathcal{J}})\mathbf{u}_{\mathcal{J}} \\ \underline{\mathbf{i}}_{\mathcal{J}} &= \mathbf{T}_{\mathcal{J}}^{-1}(\delta_{\mathcal{J}})\tilde{\mathbf{C}}\underline{\mathbf{x}},\end{aligned}\quad (15)$$

where we abbreviated

$$\begin{aligned}\tilde{\mathbf{A}} &:= \left[\mathbf{A} \otimes \mathbf{I}_2 + \mathbf{I}_n \otimes \begin{bmatrix} 0 & \check{\omega} \\ -\check{\omega} & 0 \end{bmatrix} \right], \\ \tilde{\mathbf{B}} &:= [\mathbf{B} \otimes \mathbf{I}_2], \quad \tilde{\mathbf{C}} := [\mathbf{C} \otimes \mathbf{I}_2].\end{aligned}$$

In this formulation, $\delta_{\mathcal{J}}$ is an input of the network model. Since $\delta_{\mathcal{J}}$ will not be needed anywhere else, we augment the model by (5) which results in a model of the network with inputs $\omega_{\mathcal{J}}$, $\mathbf{u}_{\mathcal{J}}$ and output $\mathbf{i}_{\mathcal{J}}$:

$$\begin{aligned}\dot{\underline{\mathbf{x}}}_{\text{net}} &= \frac{d}{dt} \begin{bmatrix} \underline{\mathbf{x}} \\ \delta_{\mathcal{J}} \end{bmatrix} = \begin{bmatrix} \tilde{\mathbf{A}}\underline{\mathbf{x}} + \tilde{\mathbf{B}}\mathbf{T}_{\mathcal{J}}(\delta_{\mathcal{J}})\mathbf{u}_{\mathcal{J}} \\ \omega_{\mathcal{J}} - \mathbf{1}_{|\mathcal{J}|}\check{\omega} \end{bmatrix} \\ \underline{\mathbf{i}}_{\mathcal{J}} &= \mathbf{T}_{\mathcal{J}}^{-1}(\delta_{\mathcal{J}})\tilde{\mathbf{C}}\underline{\mathbf{x}}.\end{aligned}\quad (16)$$

5. INVERTER AND PLANT MODEL

Fig. 1 shows the block diagram of the coupled inverters. The coupling inductance has been modelled as a line of the network. Therefore, the inverter node $v_{i \in \mathcal{J}}$ is actually inside the inverter and no loads are connected to these vertices, which justifies our indexing. Subscript f is used to denote the remaining filter parameters $L_{f,i}, C_{f,i}$, the current flowing through the filter inductance \mathbf{i}_f and the voltage over the filter \mathbf{u}_f . Reference values given by the secondary controller are denoted with superscript o. Since the secondary controller is not investigated, these inputs are assumed to be constants corresponding to the operating point of the network. Setpoints from inner control loops are denoted by superscript *. The absolute value of the voltage is denoted by \hat{u} . Subscript m is used to differentiate low-pass filtered measured values from the actual values.

Before focusing on the controllers, the inverters must be modeled. As customary in these kinds of models, we neglect the switching process of the inverters: $\mathbf{u}_f = \mathbf{u}_f^*$. The relationship between voltage decline and current flowing through the filter is described by

$$\mathbf{u}_{abc,f,i} - \mathbf{u}_{abc,i} = R_{f,i}\mathbf{i}_{abc,f,i} + L_{f,i}\frac{d\mathbf{i}_{abc,f,i}}{dt} \quad (17)$$

$$\frac{d\mathbf{u}_{abc,i}}{dt} = \frac{1}{C_{f,i}}(\mathbf{i}_{abc,f,i} - \mathbf{i}_{abc,i}), \quad i \in \mathcal{J}. \quad (18)$$

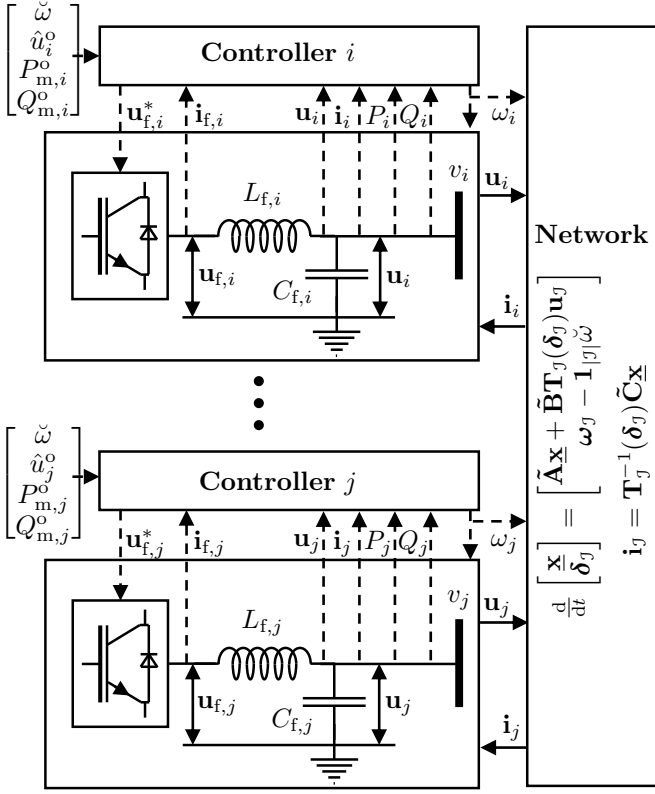


Fig. 1. Block diagram of coupled inverters

Dq-transformation, transformation to local dq-coordinates and summarizing the equations for all inverters yields

$$\frac{d\mathbf{i}_{f,j}}{dt} = \left(\mathbf{L}_f^{\circ(-1)} \otimes \begin{bmatrix} 1 \\ 1 \end{bmatrix} \right) \circ (\mathbf{u}_f - \mathbf{u}_j) + \left(\text{diag}(-\mathbf{R}_f \circ \mathbf{L}_f^{\circ(-1)}) \otimes \begin{bmatrix} 1 \\ 1 \end{bmatrix} + \text{diag}(\boldsymbol{\omega}_j) \otimes \begin{bmatrix} 0 & 1 \\ -1 & 0 \end{bmatrix} \right) \mathbf{i}_{f,j} \quad (19)$$

$$\frac{d\mathbf{u}_j}{dt} = \left(\mathbf{C}_f^{\circ(-1)} \otimes \begin{bmatrix} 1 \\ 1 \end{bmatrix} \right) \circ (\mathbf{i}_f - \mathbf{i}_j) + \left(\text{diag}(\boldsymbol{\omega}_j) \otimes \begin{bmatrix} 0 & 1 \\ -1 & 0 \end{bmatrix} \right) \mathbf{u}_j. \quad (20)$$

Equations (19) and (20) constitute a nonlinear state space model describing the filters with states \mathbf{i}_f , \mathbf{u}_j and inputs $\boldsymbol{\omega}_j$, \mathbf{u}_f , \mathbf{i}_j . Connecting this nonlinear state space model with the network state space model (16) as in Fig. 1 leads to a nonlinear model of the plant with input $\mathbf{u}_P^T = [\boldsymbol{\omega}_j^T \ \mathbf{u}_f^T]$ and state $\mathbf{x}_P^T = [\mathbf{x}^T \ \boldsymbol{\delta}_j^T \ \mathbf{i}_f^T \ \mathbf{u}_j^T]$. For the control of the inverters, we want the output to be ordered as illustrated in Fig. 2: $\mathbf{y}_P^T = [\mathbf{i}_f^T \ \mathbf{u}_j^T \ \mathbf{i}_j^T \ \mathbf{P}_j^T \ \mathbf{Q}_j^T]^T$. The output equations for \mathbf{i}_f and \mathbf{u}_j are trivial since these outputs are also states. The output equation for \mathbf{i}_j is as in (16). The values of \mathbf{P}_j and \mathbf{Q}_j are derived from \mathbf{u}_j and \mathbf{i}_j :

$$\mathbf{P}_i = \mathbf{u}_i^T \mathbf{i}_i, \quad \mathbf{Q}_i = \mathbf{u}_i^T \begin{bmatrix} 0 & -1 \\ 1 & 0 \end{bmatrix} \mathbf{i}_i, \quad i \in \mathcal{J}. \quad (21)$$

We reformulate (21) in one matrix equation:

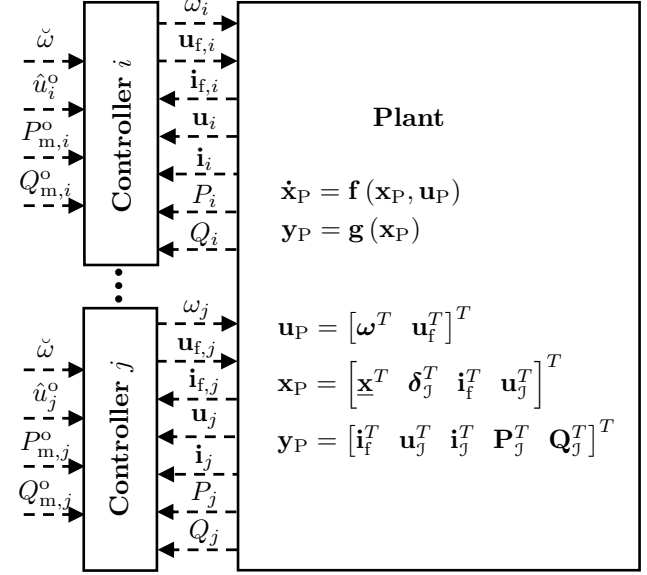


Fig. 2. Block diagram for controller design

$$\mathbf{P}_j = (\mathbf{I}_{|j|} \otimes [1 \ 1]) (\mathbf{u}_j \circ \mathbf{i}_j), \quad (22)$$

$$\mathbf{Q}_j = (\mathbf{I}_{|j|} \otimes [1 \ 1]) \left[\left((\mathbf{I}_{|j|} \otimes \begin{bmatrix} 0 & 1 \\ -1 & 0 \end{bmatrix}) \mathbf{u}_j \right) \circ \mathbf{i}_j \right].$$

With this, the nonlinear plant model

$$\dot{\mathbf{x}}_P = \mathbf{f}(\mathbf{x}_P, \mathbf{u}_P), \quad \mathbf{y}_P = \mathbf{g}(\mathbf{x}_P) \quad (23)$$

has been derived as illustrated in Fig. 2.

6. CONTROLLER STRUCTURE

6.1 Cascaded Controller

From Fig. 2 it is evident that the task is to design decentralized multiple-input multiple-output controllers. Designing such controllers without consideration of the industrial practice will be part of our future research. For now, we assume the typically used, e.g. by Pogaku et al. (2007), cascaded control structure shown in Fig. 3. The

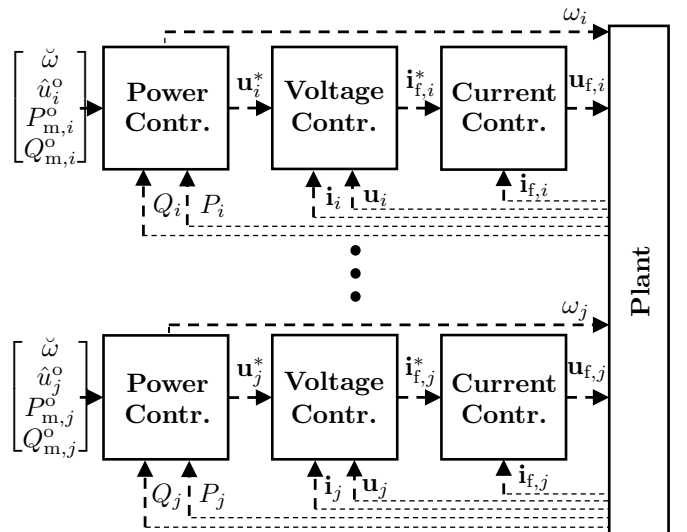


Fig. 3. Cascaded controller structure commonly used

common way to design cascaded controllers is to design the inner loops first and independently from the outer ones. The outer loops are then designed considering the inner closed loop. Here, we follow a different approach and reformulate the control design problem such that all the loops can be designed simultaneously. Then, the inner loops are designed under consideration of the outer loops.

Commonly used current controllers are described by

$$\begin{aligned} \dot{\mathbf{x}}_{CC,i} &= \mathbf{i}_{f,i}^* - \mathbf{i}_{f,i}, \\ \mathbf{u}_{f,i} &= K_{pC,i}(\mathbf{i}_{f,i}^* - \mathbf{i}_{f,i}) + K_{iC,i}\mathbf{x}_{CC,i} \\ &\quad - L_{f,i} \begin{bmatrix} 0 & \check{\omega} \\ -\check{\omega} & 0 \end{bmatrix} \mathbf{i}_{f,i}, \quad i \in \mathcal{J} \end{aligned} \quad (24)$$

and commonly used voltage controllers by

$$\begin{aligned} \dot{\mathbf{x}}_{VC,i} &= \mathbf{u}_i^* - \mathbf{u}_i, \\ \mathbf{i}_{f,i}^* &= K_{pV,i}(\mathbf{u}_i^* - \mathbf{u}_i) + K_{iV,i}\mathbf{x}_{VC,i} + F_{pV,i}\mathbf{i}_i \\ &\quad - C_{f,i} \begin{bmatrix} 0 & \check{\omega} \\ -\check{\omega} & 0 \end{bmatrix} \mathbf{u}_i, \quad i \in \mathcal{J}. \end{aligned} \quad (25)$$

For the usage in the power controller, the active and reactive power components are low-pass filtered:

$$\begin{aligned} \dot{\mathbf{P}}_m &= -\omega_c \circ \mathbf{P}_m + \omega_c \circ \mathbf{P}_j, \\ \dot{\mathbf{Q}}_m &= -\omega_c \circ \mathbf{Q}_m + \omega_c \circ \mathbf{Q}_j. \end{aligned} \quad (26)$$

Then, droop control is applied

$$\begin{aligned} \omega_j &= \check{\omega} - \mathbf{k}_P \circ \mathbf{P}_m + \mathbf{k}_P \circ \mathbf{P}_m^o \\ \mathbf{u}_j^* &= (\hat{\mathbf{u}}_j^o - \mathbf{k}_Q \circ \mathbf{Q}_m + \mathbf{k}_Q \circ \mathbf{Q}_m^o) \otimes \begin{bmatrix} 1 \\ 0 \end{bmatrix}. \end{aligned} \quad (27)$$

To summarize, there are the current controllers (24), voltage controllers (25) and power controllers (27) with the respective low-pass filters (26). The controllers are all linear and from Fig. 3 it is evident that they can be summarized to a linear state space model with input $\mathbf{u}_d^T = [\mathbf{i}_f^T \ \mathbf{u}_j^T \ \mathbf{i}_j^T \ \mathbf{P}_j^T \ \mathbf{Q}_j^T]$, reference input $\mathbf{r}_d^T = [\check{\omega}^T \ \hat{\mathbf{u}}_j^{oT} \ \mathbf{P}_m^{oT} \ \mathbf{Q}_m^{oT}]$ and output $\mathbf{y}_d^T = [\omega_j^T \ \mathbf{u}_f^T]$:

$$\begin{aligned} \dot{\mathbf{x}}_d &= \mathbf{A}_d \mathbf{x}_d + \mathbf{B}_d \mathbf{u}_d + \mathbf{F}_{1d} \mathbf{r}_d \\ \mathbf{y}_d &= \mathbf{C}_d \mathbf{x}_d + \mathbf{D}_d \mathbf{u}_d + \mathbf{F}_{2d} \mathbf{r}_d. \end{aligned} \quad (28)$$

With this, the design of the cascaded controllers has been reformulated to the design of a structurally constrained, dynamic output controller (28). From now on, the controller (28) after coordinate displacement into the operating point of the plant

$$\begin{aligned} \Delta \dot{\mathbf{x}}_d &= \mathbf{A}_d \Delta \mathbf{x}_d + \mathbf{B}_d \Delta \mathbf{u}_d \\ \Delta \mathbf{y}_d &= \mathbf{C}_d \Delta \mathbf{x}_d + \mathbf{D}_d \Delta \mathbf{u}_d \\ \mathbf{y}_d &= \Delta \mathbf{y}_d + \mathbf{y}_{d,0}, \quad \mathbf{u}_d = \Delta \mathbf{u}_d + \mathbf{u}_{d,0}, \end{aligned} \quad (29)$$

is considered, where constant reference inputs are assumed and Δ denotes the difference of the signal to the corresponding value in the operating point.

6.2 Reduction to the Design of a Static Controller

The design of (29) based on the linearized plant with the system matrices $\mathbf{A}_P, \mathbf{B}_P$ and \mathbf{C}_P can be reduced to the design of a static controller as described e.g. by Föllinger (2008). Doing so yields the augmented plant

$$\begin{aligned} \dot{\mathbf{x}}_a &= \mathbf{A}_a \mathbf{x}_a + \mathbf{B}_a \mathbf{u}_a \\ \mathbf{y}_a &= \mathbf{C}_a \mathbf{x}_a, \end{aligned} \quad (30)$$

where the abbreviations

$$\begin{aligned} \mathbf{x}_a &= \begin{bmatrix} \Delta \mathbf{x}_P \\ \Delta \mathbf{x}_d \end{bmatrix}, \quad \mathbf{u}_a = \begin{bmatrix} \Delta \dot{\mathbf{x}}_d \\ \Delta \mathbf{u}_P \end{bmatrix}, \quad \mathbf{y}_a = \begin{bmatrix} \Delta \mathbf{x}_d \\ \Delta \mathbf{y}_P \end{bmatrix}, \\ \mathbf{A}_a &= \begin{bmatrix} \mathbf{A}_P & \mathbf{0} \\ \mathbf{0} & \mathbf{0} \end{bmatrix}, \quad \mathbf{B}_a = \begin{bmatrix} \mathbf{0} & \mathbf{B}_P \\ \mathbf{I} & \mathbf{0} \end{bmatrix}, \quad \mathbf{C}_a = \begin{bmatrix} \mathbf{0} & \mathbf{I} \\ \mathbf{C}_P & \mathbf{0} \end{bmatrix} \end{aligned}$$

were used, and the static controller \mathbf{K} that needs to be designed

$$\mathbf{u}_a = \begin{bmatrix} \mathbf{A}_d & \mathbf{B}_d \\ \mathbf{C}_d & \mathbf{D}_d \end{bmatrix} \begin{bmatrix} \Delta \mathbf{x}_d \\ \Delta \mathbf{y}_P \end{bmatrix} = \mathbf{K} \mathbf{y}_a. \quad (31)$$

It is easy to recognize that the system matrices of (30) contain only matrices of the plant, while (31) contains the matrices of the dynamic controller and therefore all the tunable control parameters.

7. CONTROLLER DESIGN METHOD

The design of \mathbf{K} must respect the fixed structure of the matrices $\mathbf{A}_d, \mathbf{B}_d, \mathbf{C}_d, \mathbf{D}_d$ that result from the decentralized setup and from the usage of cascaded controllers with predefined structure for each inverter. To tune the parameters of the controllers, the direct method of Konigorski (1987b) for eigenvalue assignment is applied. Treating the intricacies of the method is beyond this work, but the basic principle will be described in what follows. The method is based on the comparison of the characteristic polynomial of the closed loop in dependence of the controller

$$P_{\mathbf{K}}(\lambda) = \det(\lambda \mathbf{I}_n - \mathbf{A}_a + \mathbf{B}_a \mathbf{K} \mathbf{C}_a)$$

with the desired characteristic polynomial defined by the desired eigenvalues $\lambda_{\mathbf{K},1}, \dots, \lambda_{\mathbf{K},n}$

$$\det(\lambda \mathbf{I}_n - \mathbf{A}_a + \mathbf{B}_a \mathbf{K} \mathbf{C}_a) \stackrel{!}{=} \prod_{i=1}^n (\lambda - \lambda_{\mathbf{K},i}).$$

This is, at least for single eigenvalues $\lambda_{\mathbf{K},i}$, equivalent to

$$\det(\lambda_{\mathbf{K},i} \mathbf{I}_n - \mathbf{A}_a + \mathbf{B}_a \mathbf{K} \mathbf{C}_a) \stackrel{!}{=} \mathbf{0}, \quad i = 1, \dots, n.$$

But the eigenvalues cannot always be arbitrarily assigned, especially in the case of decentralized control. Therefore, the functions

$$e_i(\mathbf{K}) = \det(\lambda_{\mathbf{K},i} \mathbf{I}_n - \mathbf{A}_a + \mathbf{B}_a \mathbf{K} \mathbf{C}_a), \quad i = 1, \dots, n$$

are combined into a vector

$$\mathbf{e}(\mathbf{K}) = [e_1(\mathbf{K}), \dots, e_n(\mathbf{K})]^T.$$

Then, the eigenvalue assignment problem can be solved at least approximately by minimizing

$$J = \frac{1}{2} \mathbf{e}^T \mathbf{W} \mathbf{e},$$

where \mathbf{W} is a diagonal weighting matrix. The analytic computation of the gradient $\frac{\partial J}{\partial \mathbf{K}}$, where

$$\mathbf{k} = [k_{11}, \dots, k_{1q}, k_{21}, \dots, k_{2q}, \dots, k_{p1}, \dots, k_{pq}]^T$$

contains the entries of the controller matrix \mathbf{K} , is given by Konigorski (1988). Because of the cascaded controllers, the parameters of the controller matrix \mathbf{K} cannot be tuned arbitrarily. Indeed, the optimization variables of the test network are not entries of \mathbf{K} , but entries of following vector \mathbf{r} :

$$\mathbf{r} = [\mathbf{K}_{pC}^T \ \mathbf{K}_{iC}^T \ \mathbf{K}_{pV}^T \ \mathbf{K}_{iV}^T \ \mathbf{F}_{pV}^T \ \mathbf{k}_P^T \ \mathbf{k}_Q^T \ \omega_c^T]^T.$$

The entries of \mathbf{K} therefore are functions of \mathbf{r} and the gradient given by Konigorski (1988) needs to be adapted accordingly:

Table 1. Controller parameters

	No optimization	Optimization without power sharing	Optimization with power sharing
\mathbf{K}_{pC}^T	$\begin{bmatrix} 10.5 & 10.5 & 10.5 \end{bmatrix}$	$\begin{bmatrix} 11.969 & 9.493 & 10.046 \end{bmatrix}$	$\begin{bmatrix} 11.560 & 9.943 & 10.002 \end{bmatrix}$
\mathbf{K}_{iC}^T	$\begin{bmatrix} 16\,000 & 16\,000 & 16\,000 \end{bmatrix}$	$\begin{bmatrix} 16\,957 & 15\,627 & 15\,474 \end{bmatrix}$	$\begin{bmatrix} 18\,205 & 16\,161 & 14\,049 \end{bmatrix}$
\mathbf{K}_{pV}^T	$\begin{bmatrix} 0.05 & 0.05 & 0.05 \end{bmatrix}$	$\begin{bmatrix} 0.0625 & 0.0508 & 0.0405 \end{bmatrix}$	$\begin{bmatrix} 0.0645 & 0.0510 & 0.0324 \end{bmatrix}$
\mathbf{K}_{iV}^T	$\begin{bmatrix} 390 & 390 & 390 \end{bmatrix}$	$\begin{bmatrix} 370.84 & 434.47 & 385.06 \end{bmatrix}$	$\begin{bmatrix} 272.17 & 510.11 & 380.29 \end{bmatrix}$
\mathbf{F}_{pV}^T	$\begin{bmatrix} 0.75 & 0.75 & 0.75 \end{bmatrix}$	$\begin{bmatrix} 0.7683 & 0.7635 & 0.7296 \end{bmatrix}$	$\begin{bmatrix} 0.7141 & 0.7507 & 0.7550 \end{bmatrix}$
\mathbf{k}_P^T	$10^{-6} \begin{bmatrix} 94 & 94 & 94 \end{bmatrix}$	$10^{-6} \begin{bmatrix} 12.2 & 5.8 & 38.4 \end{bmatrix}$	$10^{-6} \begin{bmatrix} 18.2 & 18.2 & 18.2 \end{bmatrix}$
\mathbf{k}_Q^T	$10^{-4} \begin{bmatrix} 13 & 13 & 13 \end{bmatrix}$	$10^{-4} \begin{bmatrix} 33.19 & 9.1 & 32.9 \end{bmatrix}$	$10^{-4} \begin{bmatrix} 21.47 & -2.3 & 11.9 \end{bmatrix}$

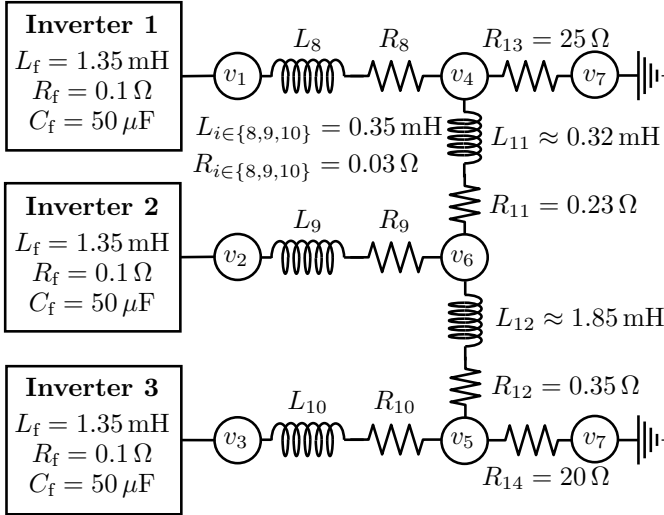


Fig. 4. Test System

$$\frac{\partial \mathbf{J}}{\partial r_i} = \frac{\partial \mathbf{J}}{\partial k_{11}} \frac{\partial k_{11}}{\partial r_i} + \frac{\partial \mathbf{J}}{\partial k_{12}} \frac{\partial k_{12}}{\partial r_i} + \dots + \frac{\partial \mathbf{J}}{\partial k_{pq}} \frac{\partial k_{pq}}{\partial r_i}.$$

8. APPLICATION AND SIMULATION

For comparability, the system described by Pogaku et al. (2007) is used and displayed in Fig. 4. An operating point close to the one used by Pogaku et al. (2007) is chosen. A slight difference in operating points is unavoidable due to the virtual resistors Pogaku et al. (2007) add between each node and ground. Starting with the controller parameters from Pogaku et al. (2007), the controller parameters are tuned to achieve a better dynamical behavior of the network. We display the resulting controller parameters

in Table 1. The corresponding closed loop eigenvalues are shown in Fig. 5. Trying to shift the dominant eigenvalues further to the left quickly shows that this can primarily be achieved by choosing larger bandwidths for the filter (26) parameters ω_c as is clear intuitively. However, the filters' task is to slow down the primary controllers such that they don't react to higher oscillations induced by the switching processes of the inverters. Since we neglected this switching process in the model, ω_c should not be changed. Fixing ω_c and trying to dampen and accelerate the slow oscillatory modes at the same time leads to the closed loop eigenvalues denoted by triangles in Fig. 5. The corresponding control parameters are given in the second column of Table I. Because all entries of \mathbf{k}_P were changed, the better transient behavior is achieved only by giving up on power sharing after a load change. Repeating the procedure while keeping the entries of \mathbf{k}_P equal, i.e. holding on to power sharing behavior after load changes, resulted in the eigenvalues denoted by squares in Fig. 5. The attempt to also dampen the oscillatory modes of higher frequencies worsened the locations of the slow oscillatory modes and was therefore not further pursued.

To demonstrate the improvement in transient behavior, the first experiment conducted by Pogaku et al. (2007) is reproduced: A step change of about 3.8 kW real power of the load connected to vertex 4. We model this by changing the load impedance from 25 Ω to 15 Ω after 0.05 s simulation time. The simulations are conducted using the nonlinear plant model, which is changed accordingly after the incident. Unlike Pogaku et al. (2007), we do not display the low-pass filtered powers $\mathbf{P}_m, \mathbf{Q}_m$, but $\mathbf{P}_J, \mathbf{Q}_J$.

Fig. 6 displays the real power output of the inverters for all three cases. With the original controller parameters, the inverters share the additional load. But, in the transition

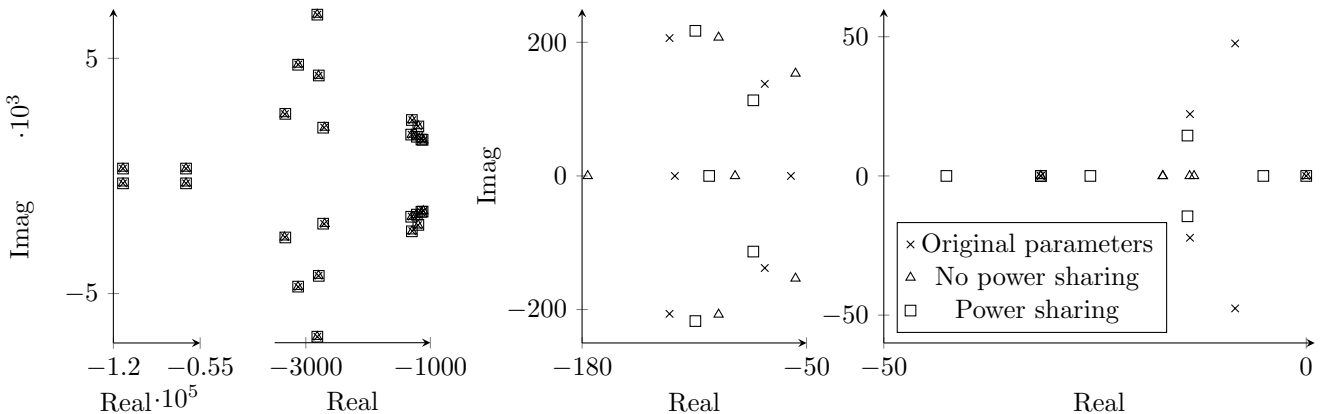


Fig. 5. Eigenvalues of the closed plant

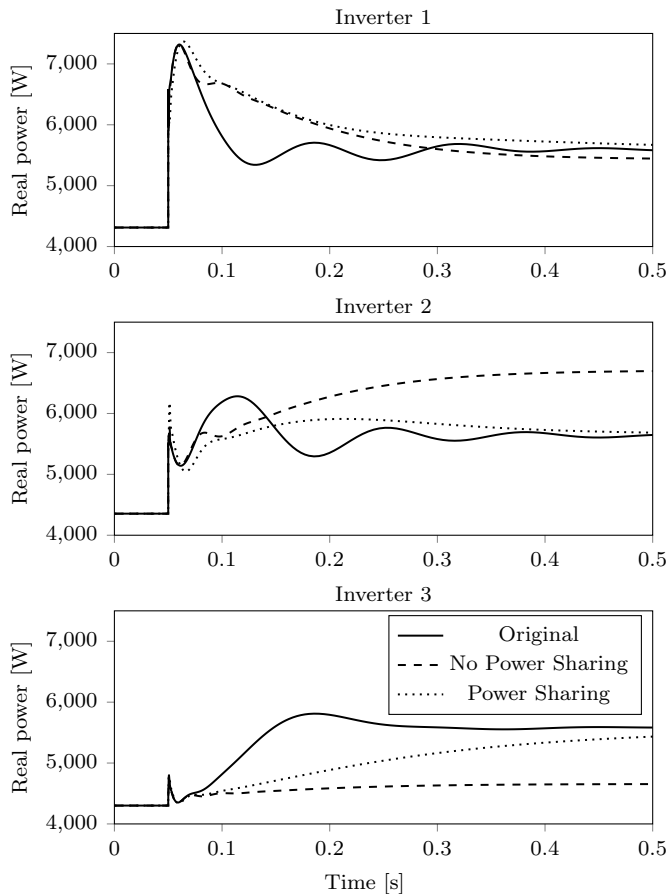


Fig. 6. Simulation of a step change of additional 3.8 kW of the load connected to vertex 4

to the new steady state, the power output of the inverters is oscillating considerably. In the second case, where the controller parameters were optimized without restricting the real power droops, the oscillations have clearly been reduced and the system response is not much slower. As discussed, the power is not shared anymore. In the third case, where the parameters were tuned while still holding on to the goal of power sharing, the system is also well dampened. The response of the third controller in this case is fairly slow, but since the goal of power sharing is not very important for short time periods, but rather in steady state, this is not much of a downside.

9. CONCLUSION AND OUTLOOK

It has been shown that the oscillations in a microgrid can be reduced considerably just by tuning the controller parameters. The overall system speed is restricted by the low-pass filter parameters ω_c , i.e. by the higher oscillations that were not modeled in this work. Still, it might be possible to enhance the system behavior even further by generating more degrees of freedom. To investigate this possibility, the commonly used controller structure with three cascaded controllers should be reconsidered. Instead, the application of general multiple-input multiple-output controllers, one for zero-level control and another for primary control, should be investigated. Especially breaking the structure of the zero-level controller seems promising. First of all, there is no need for two cascaded

PI controllers. Therefore, the dynamical order of the controller could be reduced. At the same time, the degrees of freedom could easily be increased from the five control parameter available with the common control structure $K_{pC}, K_{iC}, K_{pV}, K_{iV}, F_{pV}$ to twelve degrees of freedom of a controller matrix with six inputs and two outputs plus the degrees of freedom due to the dynamics of the controller. Since the zero-level controller uses unfiltered measurements, it is much faster than primary control. Therefore, one might also be able to dampen the faster oscillating modes, which should reduce the content of harmonics in the network and might allow to raise the bandwidths ω_c of the low-pass filters.

Also, the optimization of the control parameters had predefined eigenvalue locations as objective, which often are not crucial. Additional degrees of freedom from point of view of the optimization can be generated, when an area is specified in which the eigenvalues have to lie, instead of precise locations, e.g. Konigorski (1987a).

We designed the controllers simultaneously. This has the advantage that each controller is designed considering the other controllers. And yet, this is not necessarily the best approach, since the optimization problem that must be solved for eigenvalue assignment is not convex. With the size of the network, this drawback becomes more severe. Considering this, a better approach might be to design zero and primary controllers independently based on matched models. Besides this time-scale decomposition, other decomposition techniques like the ϵ -decomposition and the overlapping decomposition, e.g. Siljak (1991), should be considered for larger networks.

REFERENCES

- Anderson, P. and Fouad, A. (2003). *Power system control and stability*. John Wiley & Sons.
- Föllinger, O. (2008). *Regelungstechnik: Einführung in die Methoden und ihre Anwendung*. Heidelberg: Hüthig Verlag.
- Konigorski, U. (1987a). Entwurf robuster strukturbeschränkter Zustandsregelungen durch Polgebietsvorgabe mittels Straffunktionen. *Automatisierungstechnik*, 35(6), 250–254.
- Konigorski, U. (1987b). A new direct approach to the design of structurally constrained controllers. In *10th IFAC World Congress*, 265–269.
- Konigorski, U. (1988). *Ein direktes Verfahren zum Entwurf strukturbeschränkter Zustandsrückführungen durch Polvorgabe*. Düsseldorf: VDI-Verlag.
- Kundur, P. (1994). *Power system stability and control*. McGraw-Hill.
- Litz, L. (1983). *Dezentrale Regelung*. Methoden der Regelungstechnik, München: Oldenbourg Verlag.
- Lunze, J. (1992). *Feedback control of large-scale systems*. London: Prentice-Hall.
- Pogaku, N., Prodanovic, M., and Green, T.C. (2007). Modeling, analysis and testing of autonomous operation of an inverter-based microgrid. *IEEE Transactions on power electronics*, 22(2), 613–625.
- Sauer, P.W. and Pai, M. (1997). *Power System Dynamics and Stability*. London: Prentice Hall.
- Siljak, D.D. (1991). *Decentralized control of complex systems*. New York: Academic Press.